

Accelerated global warming by metabolic imbalances on Earth

Gesa A Weyhenmeyer¹

¹Ecology and Genetics/Limnology

November 23, 2022

Abstract

Global warming is presently accelerating, raising the question whether all climate forcing and feedback mechanisms have been accounted for. Here a metabolic climate forcing and feedback mechanism is introduced, providing an explanation for the observed accelerated global warming. Based on more than 400,000 meteorological observations at various latitudes, it is shown that temperatures at the Earth's surface increasingly depart from thermodynamic equilibrium conditions towards warming at all examined geographical locations because of a long-lasting imbalance between the exothermic metabolic process of ecosystem respiration and the endothermic metabolic process of photosynthesis. Following the principles of the metabolic theory, metabolic imbalances are attributed to warmer temperatures stimulating ecosystem respiration at the same time as photosynthesis becomes light constrained. Since metabolic imbalances are expected to continue until ecosystem respiration becomes substrate limited, there is an urgent need to navigate climate mitigation towards measures that can slow down ecosystem respiration.

1 **Accelerated global warming by metabolic imbalances on Earth**

2

3 Gesa A. Weyhenmeyer^{*,1}

4 ¹Department of Ecology and Genetics/Limnology, Uppsala University, 75236 Uppsala, Sweden

5

6 *Corresponding author: Gesa Weyhenmeyer, Gesa.Weyhenmeyer@ebc.uu.se, phone: +46-768383106

7

8

9 Author contribution statement: GW initiated the project, came up with all concepts, performed
10 all data analyses and wrote the paper.

11

12

13 **Key points:**

14 • A temperature departure from solar irradiance co-varies with a long-lasting imbalance
15 between photosynthesis and ecosystem respiration.

16

17 • Metabolic imbalances increase under anthropogenic global warming, causing a
18 greenhouse gas and energy accumulation in the atmosphere.

19

20 • Earth's warming and cooling events are driven by metabolic imbalances.

21

22

23

24

25

26

27 **Abstract**

28 Global warming is presently accelerating, raising the question whether all climate forcing and
29 feedback mechanisms have been accounted for. Here a metabolic climate forcing and feedback
30 mechanism is introduced, providing an explanation for the observed accelerated global warming.
31 Based on more than 400,000 meteorological observations at various latitudes, it is shown that
32 temperatures at the Earth's surface increasingly depart from thermodynamic equilibrium
33 conditions towards warming at all examined geographical locations because of a long-lasting
34 imbalance between the exothermic metabolic process of ecosystem respiration and the
35 endothermic metabolic process of photosynthesis. Following the principles of the metabolic
36 theory, metabolic imbalances are attributed to warmer temperatures stimulating ecosystem
37 respiration at the same time as photosynthesis becomes light constrained. Since metabolic
38 imbalances are expected to continue until ecosystem respiration becomes substrate limited, there
39 is an urgent need to navigate climate mitigation towards measures that can slow down ecosystem
40 respiration.

41

42 **1. Introduction**

43 The global carbon cycle plays a key role in regulating Earth's temperature with carbon-climate
44 feedback mechanisms well integrated into Earth System Models (Friedlingstein & Prentice,
45 2010). By far the largest fluxes in the global carbon cycle comprise photosynthesis and ecosystem
46 respiration (Friedlingstein et al., 2022; Masson-Delmotte et al., 2021). Both fluxes are driven by
47 the metabolic rate of individual organisms on Earth, causing energy and carbon to be frequently
48 exchanged between the atmosphere and the biosphere, thereby influencing Earth's climate
49 (Falkowski et al., 2000). According to the metabolic theory of ecology the ultimate driver for the
50 metabolic rate on Earth is temperature, following the kinetics described by the Van't Hoff-
51 Arrhenius relation (Brown et al., 2004; Gillooly et al., 2001):

$$52 \quad B_i = b_0 \cdot e^{-E_a/(k_B \cdot T)} \cdot M_i^\alpha \quad (1)$$

53 where B_i is the metabolic rate of any optional organism (measured as energy in watts or as oxygen
54 consumption or carbon dioxide production per unit time), b_0 is a normalization constant
55 independent of body size and temperature, E_a is the average activation energy in eV, k_B is the
56 Boltzmann's constant ($8.62 \cdot 10^{-5} \cdot \text{eV} \cdot \text{K}^{-1}$), T is the absolute temperature in K, M_i is body size
57 expressed as pgC and α is the allometric scaling exponent for body size.

58

59 Temperature alone is, however, not the only fundamental physical constraint on the metabolic
60 rate on Earth. Photoautotrophs can, for example, only survive when they receive sufficient energy
61 from the sun (Relyea, 2021). To account for the dependency of the photosynthetic rate on light,
62 Lopez-Urrutia et al. (2006) extended the metabolic theory of ecology by the Michaelis-Menten
63 photosynthetic light response:

$$64 \quad P_i = p_0 \cdot e^{-E_a/(k_B \cdot T)} \cdot M_i^\alpha \cdot \left(\frac{PAR}{k_m + PAR} \right) \quad (2)$$

65 where P_i is the rate of individual gross photosynthesis in $\text{mmol of O}_2 \cdot \text{d}^{-1}$, p_0 is a normalization
66 constant independent of body size, temperature and light, E_a is the average activation energy for
67 photosynthetic reactions in eV, k_B is the Boltzmann's constant ($8.62 \cdot 10^{-5} \cdot \text{eV} \cdot \text{K}^{-1}$), T is the
68 absolute temperature in K, M_i is body size expressed as pgC, α is the allometric scaling exponent
69 for autotroph body size, PAR is the daily irradiance in $\text{mol photons} \cdot \text{m}^{-2} \cdot \text{d}^{-1}$ and k_m is the
70 Michaelis-Menten half-saturation constant in $\text{mol photons} \cdot \text{m}^{-2} \cdot \text{d}^{-1}$.

71

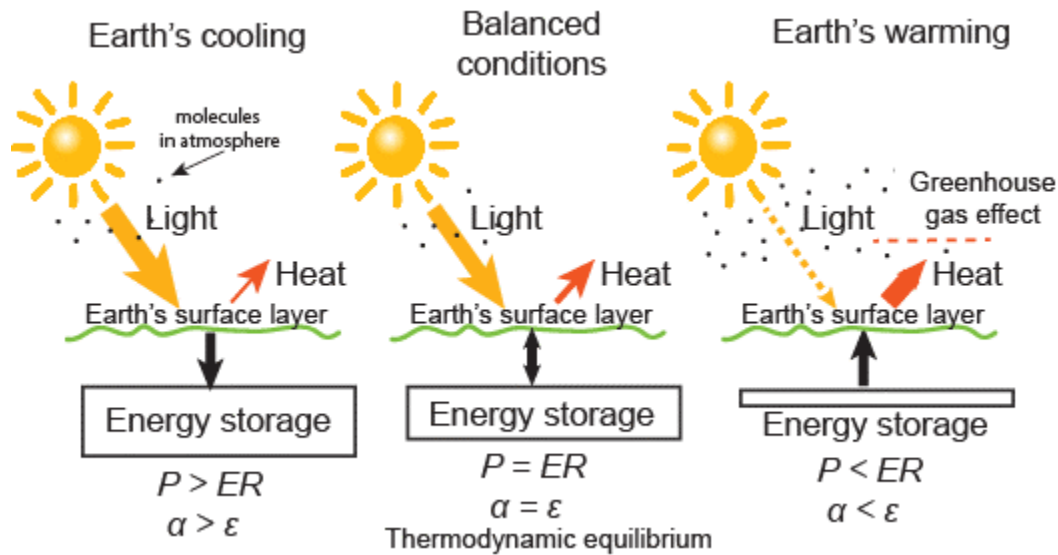
72 According to the extended metabolic theory, eq. 1 is applicable for the prediction of the
73 heterotrophic respiration rate while eq. 2 needs to be applied for the prediction of the
74 photosynthetic rate. Both rates are presently assumed to be in balance over the course of a year
75 and on the global scale, as, for example, illustrated in the annually renewed global carbon budget
76 (Friedlingstein et al., 2022; Friedlingstein et al., 2020). During a 24-hour period, it is, however,
77 well known that the rates are commonly out of balance with either photosynthesis or ecosystem
78 respiration dominating, depending on the availability of sunlight (Wilson et al., 2002). In some
79 ecosystems, respiration can even exceed photosynthesis over several years, as shown for lake
80 ecosystems in the boreal region (Cole et al., 1994; Drake et al., 2018; Raymond et al., 2013;
81 Tranvik et al., 2009). In those ecosystems, the heterotrophic respiration flux is disproportionately
82 large due to the availability of inflowing organic carbon as an extra, light-independent energy
83 source, which microorganisms are capable to efficiently utilize (Cole et al., 1994). Such long-
84 lasting metabolic imbalances with a clear dominance of the exothermic process of ecosystem
85 respiration are expected to cause a substantial greenhouse gas and temperature increase in the
86 atmospheric boundary layer, further accelerating the global warming trend.

87 Presently, it is not known where, when and for how long metabolic imbalances on Earth occur
88 and how temperatures at the Earth's surface are related to such imbalances. An imbalance

89 between the endothermic process of photosynthesis and the exothermic process of ecosystem
 90 respiration corresponds to non-equilibrium conditions at the Earth's surface. Under such
 91 conditions, not only photosynthesis (P) and ecosystem respiration (ER) are out of balance but
 92 also Earth's absorptivity (α) and emissivity (ε). A comparison between the P/ER and the α/ε ratio
 93 is relevant for the understanding of Earth's temperature for various reasons. Both ratios describe
 94 how light reaching the Earth's surface can finally be transformed to heat. Under thermodynamic
 95 equilibrium conditions, the light-to-heat ratio at the Earth's surface follows the principles of the
 96 Stefan-Boltzmann law, and all ratios receive a value of one (Fig. 1):

$$\begin{array}{l}
 \text{Earth's metabolism} \quad \text{Kirchhoff's law} \quad \text{Stefan-Boltzmann law} \\
 \frac{\overline{P}}{ER} = \frac{\overline{\alpha}}{\varepsilon} = \frac{\overline{G_s}}{T_s^4 \cdot \sigma} = 1 \quad (3)
 \end{array}$$

98 where P is the photosynthetic rate in W, ER is the ecosystem respiration rate in W, α is the
 99 absorptivity of the Earth's surface, ε is the emissivity of the Earth's surface, G_s is the solar
 100 irradiance at the Earth's surface in $W \cdot m^{-2}$, T_s is the absolute temperature at the Earth's surface in
 101 K and σ is the Stefan-Boltzmann constant in $W \cdot m^{-2} \cdot K^{-4}$.



102
 103 **Figure 1. Concept of Earth's cooling and warming.** Whenever sufficient light reaches the Earth's
 104 surface, photosynthesis (P) commonly exceeds ecosystem respiration (ER) and absorptivity (α) exceeds
 105 emissivity (ε). Under such conditions energy is stored in the Earth's surface layer in form of heat and
 106 organic carbon. When solar irradiance decreases to critical low values, P and α become light constraint.
 107 Under those conditions, ER becomes larger than P and α larger than ε , implying that the stored energy in
 108 the Earth's surface layer is consumed and released into the atmospheric boundary layer with a consequent
 109 warming effect.

110

111 With decreasing light reaching the Earth's surface, which is not only driven by the solar cycle
112 but also strongly by the amount and characteristics of molecules in the atmosphere (Lacis et al.,
113 1981; Masson-Delmotte et al., 2021), P and α can become light constraint. Under light limitation
114 the exothermic process of ecosystem respiration as well as the emission of heat from the Earth's
115 surface can potentially continue until all stored energy in form of heat or organic carbon in the
116 Earth's surface layer is depleted, resulting in a net heat and greenhouse gas flux from the Earth's
117 surface into the atmosphere, with a consequent warming of the atmospheric boundary layer (Fig.
118 1).

119

120 Assuming that light-to-heat transformation processes at the Earth's surface such as
121 photosynthesis and ecosystem respiration as well as Earth's absorptivity and emissivity co-vary
122 due to their direct dependency on the solar cycle, it is hypothesized that variations in those
123 processes determine in how far temperature departs from thermodynamic equilibrium conditions
124 and the principles of the Stefan-Boltzmann law as follows:

$$\frac{\overline{P}}{ER} = \frac{\overline{G_s}}{T_s^4 \cdot \sigma} \quad (4)$$

126 where P is the photosynthetic rate in W, ER is the ecosystem respiration rate in W, G_s is the solar
127 irradiance at the Earth's surface in $W \cdot m^{-2}$, T_s is the absolute temperature at the Earth's surface in
128 K and σ is the Stefan-Boltzmann constant in $W \cdot m^{-2} \cdot K^{-4}$.

129

130 To test the hypothesis more than 400,000 meteorological observations at the Earth's surface at
131 various latitudes were used, where the P/ER ratio was determined by applying the main principles
132 of the extended metabolic theory of ecology.

133

134 **2. Methods**

135 **2.1. Identification of metabolic imbalances**

136 The balance between P and ER is, according to the extended theory by Lopez-Urrutia et al.,
137 (2006), a direct function of the Michaelis-Menten photosynthetic light response, or in a wider
138 sense, a direct function of solar irradiance. The P/ER ratio is here seen as a reversible chemical

139 reaction at the Earth's surface which goes into the direction of the endothermic process of P with
140 values above one when solar irradiance exceeds an equilibrium constant or into the direction of
141 the exothermic process of ER with values less than one when solar irradiance is smaller than the
142 equilibrium constant. Thus, based on metabolic theory and basic chemistry, the P/ER ratio is here
143 expressed as:

$$144 \frac{P}{ER} = \frac{G_s}{k_{eq}} \quad (5)$$

145 where P is the photosynthetic rate in W , ER is the ecosystem respiration rate in W , G_s is the solar
146 irradiance at the Earth's surface in $W \cdot m^{-2}$ and k_{eq} is the thermodynamic equilibrium constant in
147 $W \cdot m^{-2}$.

148

149 With a known thermodynamic equilibrium constant and available solar irradiance data eq. 5
150 allows to determine metabolic imbalances at any particular location and any particular time in
151 the world. Although the determination of metabolic imbalances at a particular time of the year
152 might be of interest, it is rather the identification of long-term metabolic imbalances which
153 provides most value for the understanding of global warming. For such an identification, the data
154 distribution over an entire year needs to be considered, which in this study corresponded to an
155 evaluation of annual mean values of $\left(\frac{G_s}{k_{eq}}\right)$.

156

157 **2.2. Data material and analyses**

158 Metabolic imbalances as well as temperature departures from thermodynamic equilibrium
159 conditions were examined by using hourly solar irradiance and air temperature data from the
160 Swedish Meteorological and Hydrological Institute (SMHI) and the National Aeronautics and
161 Space Administration (NASA). The examination began with observational data from SMHI, for
162 which three locations were chosen, representing a large range of latitudes: Kiruna in the North of
163 Sweden (decimal degrees: 67.83 N, 20.34 E; altitude: 459 m; station number: 180940), Östersund
164 in the central part of Sweden (decimal degrees: 63.20 N and 14.49 E; altitude: 356 m; station
165 number: 134110) and Växjö in the southern part of Sweden (decimal degrees: 56.85 N and 14.83
166 E; altitude: 199 m; station number: 64510). Hourly air temperature data for these locations,
167 measured 2 m above ground, were downloaded from:

168 <https://www.smhi.se/data/meteorologi/ladda-ner-meteorologiska->

169 [observationer/#param=airtemperatureInstant,stations=all](#). To get homogenous datasets, data were
170 taken from 2008 to 2021 (January 1 to December 31). All data were quality checked by SMHI. In
171 addition to observational air temperature data, observational global irradiance data in $\text{W}\cdot\text{m}^{-2}$ were
172 downloaded for the three locations from: [https://www.smhi.se/data/meteorologi/ladda-ner-](https://www.smhi.se/data/meteorologi/ladda-ner-meteorologiska-observationer/#param=globalIrradians,stations=all)
173 [meteorologiska-observationer/#param=globalIrradians,stations=all](#). Measurements were
174 performed using a pyranometer. All irradiance data were quality checked by SMHI. In total
175 367,917 quality checked hourly air temperature and global irradiance observational data were
176 available and used in this study.

177
178 The results from Sweden were then validated with data from North America, available as gridded
179 data from <https://power.larc.nasa.gov/data-access-viewer/>. The downloaded data represented a
180 wide variety of landscapes and latitudes with one randomly chosen site located in Texas, one in
181 the Appalachian Mountains in Pennsylvania and one in northern Ontario. For parameter
182 description and methodology of the data from North America it is referred to the description by
183 NASA at <https://power.larc.nasa.gov/data-access-viewer/>. From North America, altogether 52,614
184 hourly data during 2020-2021 (January 1 to December 31) were downloaded.

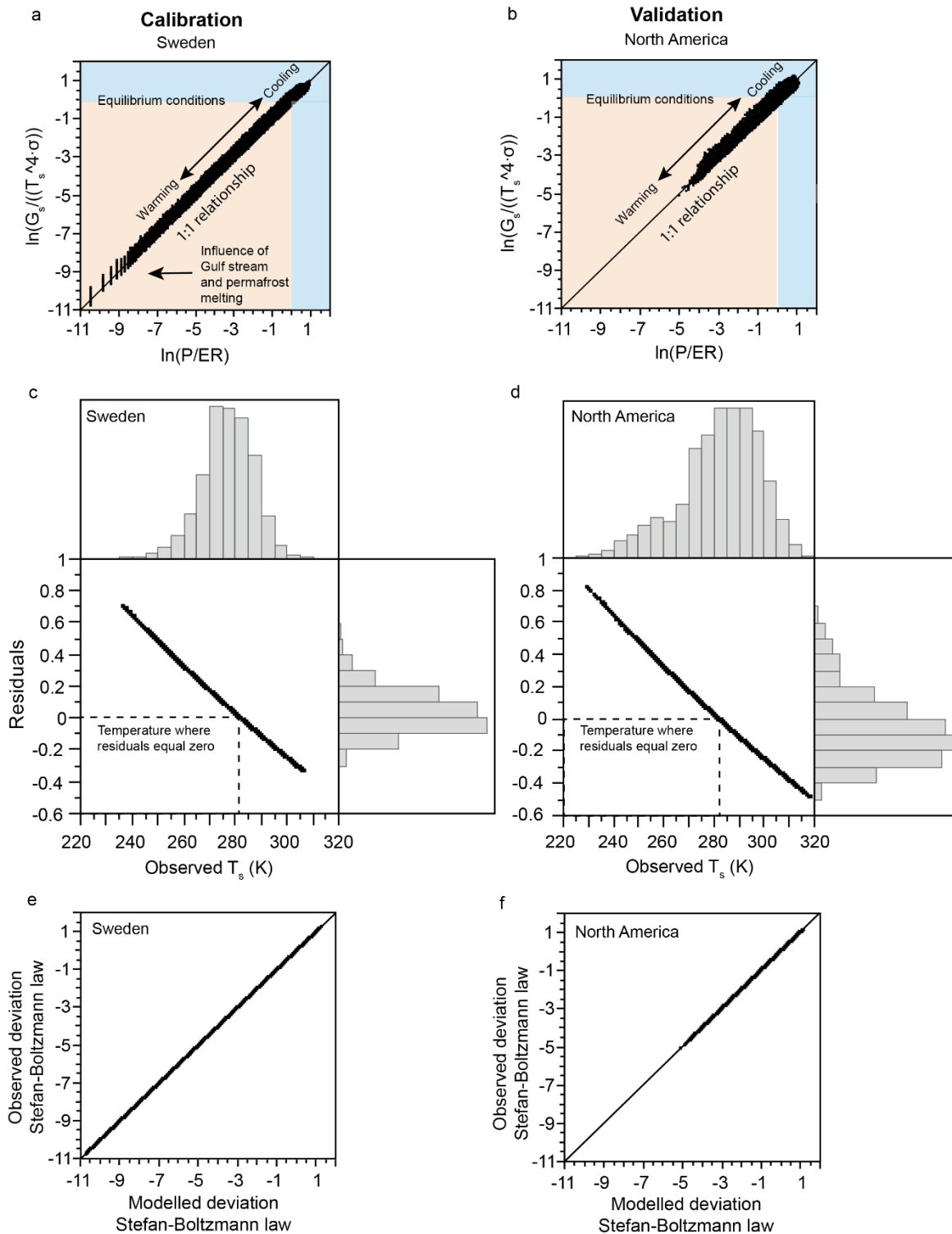
185
186 All data analyses were performed in JMP, version 15.2.0., SAS Institute Inc.

187 188 **3. Results**

189 **3.1. Metabolic imbalances and temperature departures from thermodynamic equilibrium** 190 **conditions**

191 Using more than 300,000 hourly solar irradiance and air temperature observations along a
192 latitudinal gradient in Sweden, a 1:1 relationship between the P/ER ratio, expressed by applying
193 eq. 5, and a temperature departure from thermodynamic dynamic equilibrium conditions and the
194 principles of the Stefan-Boltzmann law as outlined in eq. 4 was achieved by choosing a
195 thermodynamic equilibrium constant of $359 \text{ W}\cdot\text{m}^{-2}$. Due to residuals being strongly skewed a
196 natural logarithmic relationship was applied, giving a R^2 value of 0.998, an intercept close to zero
197 and a slope of 0.98 (Fig. 2a). Validation with more than 52,000 hourly meteorological data from
198 North America and using the same value for the equilibrium constant, i.e. $359 \text{ W}\cdot\text{m}^{-2}$, confirmed
199 a direct interaction between Earth's metabolism and the Earth's climate system as described by

200 eq. 4 (Fig. 2b). Changing the value of k_{eq} neither changed the predictive power of the model nor
201 the value of the slope but caused the intercept to increasingly deviate from zero. A k_{eq} value of
202 $359 \text{ W}\cdot\text{m}^{-2}$ resulted in the smallest intercept at all meteorological sites and during all years.
203 However, despite intercepts very close to zero there were slight variations in the intercept among
204 years and among sites, implying small variations in the equilibrium constant. Variations in k_{eq}
205 can be a consequence of stressed equilibrium conditions, which according to the Le Châtelier's
206 principle can cause shifts in equilibrium conditions.



207

208 **Figure 2. Variations in hourly light-temperature relations at six sites with contrasting land-cover in**
 209 **relation to metabolic imbalances (Sweden: Kiruna, Östersund, Växjö; North America: Ontario,**
 210 **Pennsylvania, Texas). Light-temperature relations are based on the Stefan-Boltzmann law ($G_s/T_s^4\sigma$ where**

211 G_s is the solar irradiance at the Earth's surface in $\text{W}\cdot\text{m}^{-2}$, T_s is the absolute temperature at the Earth's surface
 212 in K, σ is the Stefan-Boltzmann constant in $\text{W}\cdot\text{m}^{-2}\cdot\text{K}^{-4}$) and metabolic imbalances are expressed as the ratio
 213 between photosynthesis (P) and ecosystem respiration (ER), modelled as a function of solar irradiance (see
 214 eq. 5). **(a), (b)**. Linear relationships between modelled metabolism and observed light-temperature relations
 215 at the Earth's surface ($R^2 = 0.998$, $p < 0.0001$ for Sweden, for which the model was calibrated and $R^2 =$
 216 0.970 , $p < 0.0001$ for North America, for which the model was validated). Whenever there was a metabolic
 217 imbalance ($P > ER$ and $P < ER$, respectively), the light-temperature relation deviated from the Stefan
 218 Boltzmann law. Equilibrium conditions, where P equaled ER , were reached at $359 \text{ W}\cdot\text{m}^{-2}$. **(c), (d)** Model
 219 residuals from panels a and b, respectively, in relation to observed temperatures at the Earth's surface. **(e)**,
 220 **(f)** Final metabolic-theory based climate forcing and feedback model where results from panels a to d were
 221 combined (see eq. 4 for exact model description).

222 Although the prediction of a temperature departure from thermodynamic equilibrium conditions
 223 at the Earth's surface was powerful with R^2 values ranging between 0.966 and 0.998 at sites with
 224 highly varying land cover across Sweden and North America (Fig. 2a-b), there were deviations
 225 from a perfect 1:1 relationship. The residuals from a 1:1 relationship shifted from being positive
 226 to becoming negative, showing a perfect inverse relationship to temperature (Fig. 2c-d). A perfect
 227 inverse relationship to temperature is an indication of a temperature induced increase in kinetic
 228 energy, which is supported by the fact that the residuals could to 100 % be described by applying
 229 the concept of the Boltzmann factor (1:1 relationship with an R^2 value of 1):

$$230 \text{ Model residuals} = \ln\left(\left(\frac{E_a}{k_B \cdot T_s}\right)^4\right) = \ln\left(\left(\frac{T_0}{T_s}\right)^4\right) \quad (6)$$

231 where E_a is the activation energy, here with a value of 0.024 eV, k_B is the Boltzmann's constant
 232 ($8.62 \cdot 10^{-5} \cdot \text{eV}\cdot\text{K}^{-1}$), T_s is the absolute temperature at the Earth's surface in K, and T_0 is the
 233 temperature when model residuals equaled zero which was the case at 282 K (Fig. 2c-d). In the
 234 equation the natural logarithm was used since model residuals were given as logarithmic values.
 235 In addition, the fourth power of temperature was used, which is a result of the model structure,
 236 where the Stefan-Boltzmann law has been applied.

237

238 Combining all results gave a full explanation of observed solar irradiance-temperature relations
 239 at the Earth's surface at any particular location and any particular time by consideration of
 240 metabolic processes (1:1 relationship with an R^2 value of 1; Fig. 2e-f):

$$\overbrace{\ln\left(\frac{G_s}{T_s^4 \cdot \sigma}\right)}^{\text{Observed}} = \overbrace{\ln\left(\frac{G_s}{k_{eq}}\right)}^{\text{Climate forcing}} + \overbrace{\ln\left(\left(\frac{T_o}{T_s}\right)^4\right)}^{\text{Feedback}} \quad (7)$$

242 where G_s is the solar irradiance at the Earth's surface in $\text{W}\cdot\text{m}^{-2}$, T_s is the absolute temperature at
 243 the Earth's surface in K, σ is the Stefan-Boltzmann constant in $\text{W}\cdot\text{m}^{-2}\cdot\text{K}^{-4}$, k_{eq} is the equilibrium
 244 constant for processes at the Earth's surface in $\text{W}\cdot\text{m}^{-2}$ corresponding to $359 \text{ W}\cdot\text{m}^{-2}$, T_o is the
 245 temperature when the temperature feedback equaled zero which was the case at 282 K.

246

247

248 **3.2. Occurrence of long-lasting metabolic imbalances**

249 For the determination of long-lasting metabolic imbalances annual-mean values of $\ln\left(\frac{G_s}{k_{eq}}\right)$ were
 250 analyzed. The use of the logarithm resulted from the best model performance (eq. 7), where
 251 values larger or smaller than zero were considered as metabolic imbalances. The use of the
 252 logarithm implied that conditions during complete darkness were neglected which from a
 253 theoretical point of view is logical as there would not be any absorptivity and photosynthesis
 254 during complete darkness. However, if darkness persists only for a short time, ecosystem
 255 respiration and heat emission can still be ongoing until the energy storage in the Earth's surface
 256 layer is depleted. Thus, in this study estimates of long-lasting metabolic imbalances are rather
 257 under- than overestimated. Nevertheless, annual-mean values of $\ln\left(\frac{G_s}{k_{eq}}\right)$ at all examined sites
 258 and for all examined years remained always less than zero, reflecting a long-lasting imbalance
 259 between photosynthesis and ecosystem respiration. The lowest annual-mean values, ranging
 260 between -2.19 and -2.47, were all observed in Kiruna in northern Sweden. Kiruna is located in a
 261 geographical region with access to a large amount of light-independent energy, i.e. at this location
 262 extra heat is received from the Gulf Stream (Oort, 1964), and permafrost melting gives access to
 263 a large amount of organic carbon, stimulating the exothermic process of ecosystem respiration
 264 (Schuur et al., 2015).

265

266 **4. Discussion**

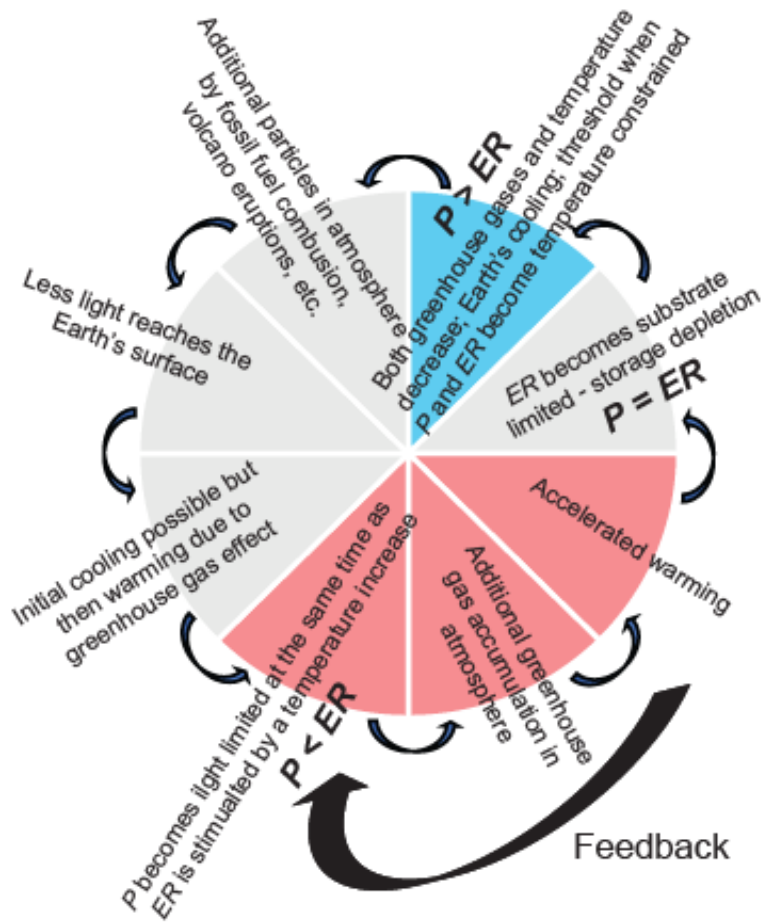
267 The results of this study support the hypothesis that Earth's metabolism directly interacts with
 268 the Earth's climate system where a 1:1 relationship between the P/ER ratio and the solar

269 irradiance-temperature relation at the Earth's surface could be established (Fig. 2). The main
270 findings are based on the extended metabolic theory of ecology, which states that the ultimate
271 drivers of the metabolic rate on Earth are sunlight and temperature (Lopez-Urrutia et al., 2006).
272 Thus, whenever sunlight and temperature are in balance, following the principles of the Stefan
273 Boltzmann law, also photosynthesis and ecosystem respiration are in balance.

274

275 At present, temperatures are, however, not any longer in balance with solar irradiance, as there
276 were substantial long-term temperature departures from thermodynamic equilibrium conditions
277 towards warming (Fig. 2a-b). The ongoing temperature departure from thermodynamic
278 equilibrium conditions is well known as the greenhouse gas driven global warming trend
279 (Masson-Delmotte et al., 2021). When temperature on Earth increases, also metabolic rates on
280 Earth increase according to the metabolic theory of ecology (Brown et al., 2004; Schramski et
281 al., 2015). Despite a stimulation of both the photosynthetic and the respiration rate by increasing
282 temperature, globally also seen in an overall greening trend of the Arctic under global warming
283 (Myers-Smith et al., 2020), ecosystem respiration can profit more from a temperature increase
284 due to a light constrain on photosynthesis during many hours of a year. Thus, there is a threshold
285 when the photosynthetic rate switches from being temperature to becoming light constrained
286 (Fig. 3). Under light constrains which here were identified to begin when solar irradiance is less
287 than $359 \text{ W}\cdot\text{m}^{-2}$, ecosystem respiration exceeds photosynthesis, causing a net energy and
288 greenhouse gas flux from the biosphere into the atmosphere, further accelerating global warming.
289 The worst-case scenario for accelerated global warming is the combination of low light and high
290 temperature. Under such conditions organic carbon will rapidly be consumed with further
291 greenhouse gas accumulation in the atmosphere, further accelerating warming. The concept of
292 higher reaction rates with increasing temperature is here defined as the climate feedback
293 mechanism (Fig. 3). The concept is supported by a modelling approach showing that carbon
294 turnover rates in ecosystems substantially increase in a warmer climate (Carvalhais et al., 2014).
295 A higher reaction rate can put a lot of pressure on equilibrium conditions, suggesting that the
296 equilibrium constant k_{eq} might be subjected to small changes, following the Le Châtelier's
297 principle.

Metabolic climate forcing and feedback mechanism



298

299 **Figure. 3. Principles of the Earth's climate system, here introduced as the metabolic climate forcing**
 300 **and feedback mechanism.** Because of a greenhouse gas effect, heat is accumulated in the atmospheric
 301 boundary layer which stimulates the ecosystem respiration rate more than the photosynthetic rate, due to
 302 a fundamental light constrain on photosynthesis. A faster ecosystem respiration rate causes an increased
 303 greenhouse gas accumulation in the atmosphere, with a consequent accelerated warming, which gives a
 304 climate feedback. The red color indicates the present accelerated global warming trend whereas the blue
 305 color indicates cooling events in Earth's history, including ice ages when both photosynthesis and
 306 ecosystem respiration become temperature constrained. The metabolic climate forcing and feedback
 307 mechanism demonstrates that Earth's cooling and warming events are driven by a switch in the main
 308 constraints on Earth's metabolism: when Earth's cools temperature is the main constrain, when Earth's
 309 warms light is the main constrain. A switch between warming and cooling events is caused by substrate
 310 limitation for ecosystem respiration and a switch between cooling and warming by additional particles
 311 and greenhouse gases in the atmosphere from e.g. volcano eruptions and fossil fuel combustion.

312 Unless there will be a substantial increase in light reaching the Earth's surface, which is unlikely
313 to happen in near future, in particular when taking the strong water vapor climate feedback
314 mechanism into account (Held & Soden, 2000), the large amounts of available light-independent
315 energy resources stored in the Earth's surface layer will make it difficult to turn around the
316 ongoing warming trend. Reversing the general long-lasting warming trend before there is a
317 depletion of the stored energy in the Earth's surface becomes even more difficult considering
318 that a dominance of ecosystem respiration causes a continued greenhouse gas accumulation in
319 the atmosphere, keeping the process of global warming alive. Support for the existence of long-
320 lasting metabolic imbalances in Earth's history is given by a recent study of Jian et al. (2022)
321 who found historically inconsistent productivity and respiration fluxes in the terrestrial global
322 carbon cycle. Also Yvon-Durocher et al. (2010) described a metabolic imbalance with warming,
323 based on experimental aquatic mesocosm work. In addition, the observed changes in the annual
324 carbon dioxide concentration amplitude in the atmosphere (Forkel et al., 2016; Wu & Lynch,
325 2000) are a clear indication of a change in the P/ER ratio although it remains open whether it is
326 photosynthesis exceeding ecosystem respiration as previously suggested or whether it is
327 ecosystem respiration which exceeds photosynthesis. According to the results of this study it is
328 the ecosystem respiration which exceeds photosynthesis.

329
330 A direct interaction between Earth's metabolism and Earth's climate, here introduced as the
331 metabolic climate forcing and feedback mechanism (Fig. 3), has been considered previously but
332 Earth System Models and the global carbon budget still assume that photosynthesis and
333 ecosystem are balanced over the course of a year. Since we presently observe long-lasting non-
334 equilibrium conditions with a shift towards the exothermic process of ecosystem respiration
335 climate change studies need to consider thermodynamic non-equilibrium conditions. Here, it was
336 clearly shown that we presently experience widespread metabolic imbalances on Earth with an
337 accelerated temperature increase as a consequence. To counteract ongoing metabolic imbalances
338 ecosystem respiration needs to be slowed down, in particular in the regions where ecosystem
339 respiration exceeds photosynthesis the most. The approach in this study allows to easily identify
340 regions and the kind of land-use where metabolic imbalances are most pronounced. Developing
341 and performing climate mitigation strategies for those regions will help to decrease the ongoing
342 net energy and greenhouse gas flux from the biosphere to the atmosphere.

343 **Acknowledgements**

344 This work has partly been financed by the Swedish Research Council (VR; Grant No. 2020-
345 03222) and the Swedish Research Council for Environment, Agricultural Sciences and Spatial
346 Planning (FORMAS; Grant No. 2020-01091). Many thanks go to panel members of the ERC-
347 Advanced Grant and to students asking all kind of challenging questions, to the Bergman Estate
348 on Fårö Foundation for funding a retreat for manuscript preparation and to James H. Brown and
349 a large number of colleagues for stimulating conversations concerning the metabolic theory of
350 ecology.

351

352 **Data Availability Statement:** All data used in this study are downloaded from public, permanent
353 sources, such as the Swedish Meteorological and Hydrological Institute
354 (<https://www.smhi.se/data/meteorologi/ladda-ner-meteorologiska-observationer>) and NASA
355 (<https://power.larc.nasa.gov/data-access-viewer/>). The downloaded data used for model
356 calibration and validation and presented in figure 2 are available as supplementary material.

357

358

359 **References**

- 360 Brown, J. H., Gillooly, J. F., Allen, A. P., Savage, V. M., & West, G. B. (2004). Toward a metabolic
361 theory of ecology. *Ecology*, *85*(7), 1771-1789. <Go to ISI>://WOS:000223113500001
- 362 Carvalhais, N., Forkel, M., Khomik, M., Bellarby, J., Jung, M., Migliavacca, M., et al. (2014).
363 Global covariation of carbon turnover times with climate in terrestrial ecosystems.
364 *Nature*, *514*(7521), 213-+. <Go to ISI>://WOS:000342663100039
- 365 Cole, J. J., Caraco, N. F., Kling, G. W., & Kratz, T. K. (1994). Carbon-dioxide supersaturation in the
366 surface waters of lakes. *Science*, *265*(5178), 1568-1570. <Go to ISI>://A1994PF33600031
- 367 Drake, T. W., Raymond, P. A., & Spencer, R. G. M. (2018). Terrestrial carbon inputs to inland
368 waters: A current synthesis of estimates and uncertainty. *Limnology and Oceanography*
369 *Letters*, *3*(3), 132-142.
370 <https://aslopubs.onlinelibrary.wiley.com/doi/abs/10.1002/lol2.10055>

371 Falkowski, P., Scholes, R. J., Boyle, E., Canadell, J., Canfield, D., Elser, J., et al. (2000). The global
372 carbon cycle: A test of our knowledge of earth as a system. *Science*, 290(5490), 291-296.
373 Review. <Go to ISI>://WOS:000089818100034

374 Forkel, M., Carvalhais, N., Rodenbeck, C., Keeling, R., Heimann, M., Thonicke, K., et al. (2016).
375 Enhanced seasonal CO₂ exchange caused by amplified plant productivity in northern
376 ecosystems. *Science*, 351(6274), 696-699. <Go to ISI>://WOS:000369810000037

377 Friedlingstein, P., Jones, M. W., O'Sullivan, M., Andrew, R. M., Bakker, D. C. E., Hauck, J., et al.
378 (2022). Global Carbon Budget 2021. *Earth System Science Data*, 14(4), 1917-2005. <Go
379 to ISI>://WOS:000787247700001

380 Friedlingstein, P., O'Sullivan, M., Jones, M. W., Andrew, R. M., Hauck, J., Olsen, A., et al. (2020).
381 Global Carbon Budget 2020. *Earth System Science Data*, 12(4), 3269-3340. <Go to
382 ISI>://WOS:000599511400001

383 Friedlingstein, P., & Prentice, I. C. (2010). Carbon-climate feedbacks: a review of model and
384 observation based estimates. *Current Opinion in Environmental Sustainability*, 2(4), 251-
385 257. <Go to ISI>://WOS:000283805300008

386 Gillooly, J. F., Brown, J. H., West, G. B., Savage, V. M., & Charnov, E. L. (2001). Effects of size and
387 temperature on metabolic rate. *Science*, 293(5538), 2248-2251. <Go to
388 ISI>://WOS:000171139400042

389 Held, I. M., & Soden, B. J. (2000). Water vapor feedback and global warming. *Annual Review of*
390 *Energy and the Environment*, 25, 441-475. <Go to ISI>://WOS:000166624500014

391 Jian, J., Bailey, V., Dorheim, K., Konings, A. G., Hao, D., Shiklomanov, A. N., et al. (2022).
392 Historically inconsistent productivity and respiration fluxes in the global terrestrial
393 carbon cycle. *Nature Communications*.

394 Lacis, A., Hansen, J., Lee, P., Mitchell, T., & Lebedeff, S. (1981). Greenhouse-effect of trace
395 gases, 1970-1980. *Geophysical Research Letters*, 8(10), 1035-1038. <Go to
396 ISI>://WOS:A1981MN15000003

397 Lopez-Urrutia, A., San Martin, E., Harris, R. P., & Irigoien, X. (2006). Scaling the metabolic
398 balance of the oceans. *Proceedings of the National Academy of Sciences of the United*
399 *States of America*, 103(23), 8739-8744. <Go to ISI>://WOS:000238278400030

400 Masson-Delmotte, V., Zhai, P., Pirani, A., Connors, S. L., Péan, C., Berger, S., et al. (2021). *IPCC,*
401 *2021: Climate Change 2021: The Physical Science Basis. Contribution of Working Group I*
402 *to the Sixth Assessment Report of the Intergovernmental Panel on Climate Change.*
403 Cambridge, United Kingdom and New York, NY, USA: Cambridge University Press.

404 Myers-Smith, I. H., Kerby, J. T., Phoenix, G. K., Bjerke, J. W., Epstein, H. E., Assmann, J. J., et al.
405 (2020). Complexity revealed in the greening of the Arctic. *Nature Climate Change*, *10*(2),
406 106-117. <Go to ISI>://WOS:000512150200006

407 Oort, A. H. (1964). Computations of the eddy heat and density transports across the Gulf
408 stream. *Tellus*, *16*(1), 55-63. <Go to ISI>://WOS:A1964XF68600008

409 Raymond, P. A., Hartmann, J., Lauerwald, R., Sobek, S., McDonald, C., Hoover, M., et al. (2013).
410 Global carbon dioxide emissions from inland waters. *Nature*, *503*(7476), 355-359. <Go to
411 ISI>://WOS:000327163200032

412 Relyea, R. (2021). *Ecology - The Economy of Nature*. New York, USA: Macmillan Learning.

413 Schramski, J. R., Dell, A. I., Grady, J. M., Sibly, R. M., & Brown, J. H. (2015). Metabolic theory
414 predicts whole-ecosystem properties. *Proceedings of the National Academy of Sciences*
415 *of the United States of America*, *112*(8), 2617-2622. <Go to
416 ISI>://WOS:000349911700076

417 Schuur, E. A. G., McGuire, A. D., Schadel, C., Grosse, G., Harden, J. W., Hayes, D. J., et al. (2015).
418 Climate change and the permafrost carbon feedback. *Nature*, *520*(7546), 171-179. <Go
419 to ISI>://WOS:000352454600029

420 Tranvik, L. J., Downing, J. A., Cotner, J. B., Loiselle, S. A., Striegl, R. G., Ballatore, T. J., et al.
421 (2009). Lakes and reservoirs as regulators of carbon cycling and climate. *Limnology and*
422 *Oceanography*, *54*(6), 2298-2314. <Go to ISI>://000272785700003

423 Wilson, K., Goldstein, A., Falge, E., Aubinet, M., Baldocchi, D., Berbigier, P., et al. (2002). Energy
424 balance closure at FLUXNET sites. *Agricultural and Forest Meteorology*, *113*(1-4), 223-
425 243. <Go to ISI>://WOS:000179188300012

426 Wu, W. L., & Lynch, A. H. (2000). Response of the seasonal carbon cycle in high latitudes to
427 climate anomalies. *Journal of Geophysical Research-Atmospheres*, *105*(D18), 22897-
428 22908. <Go to ISI>://WOS:000089598000016

429 Yvon-Durocher, G., Jones, J. I., Trimmer, M., Woodward, G., & Montoya, J. M. (2010). Warming
430 alters the metabolic balance of ecosystems. *Philosophical Transactions of the Royal*
431 *Society B-Biological Sciences*, 365(1549), 2117-2126. <Go to
432 ISI>://WOS:000278163800012
433